

Synthesis and Study of Physicochemical Properties of New Substituted Tetrathieno[2,3-*b*]porphyrazines

Tatiana V. Dubinina,^{a,b} Daria V. Dyumaeva,^a Stanislav A. Trashin,^b Marina V. Sedova,^c Alexey B. Karpo,^d Vitaly I. Krasovskii,^d and Larisa G. Tomilova^{a,b}

^aDepartment of Chemistry, M.V. Lomonosov Moscow State University, 119991 Moscow, Russian Federation

^bInstitute of Physiologically Active Compounds, Russian Academy of Sciences, 142432 Chernogolovka, Moscow Region, Russian Federation

^cInstitute for Theoretical and Applied Electromagnetics, Russian Academy of Sciences, 125412 Moscow, Russian Federation

^dA.M. Prokhorov Institute of General Physics, Russian Academy of Sciences, 119991 Moscow, Russian Federation

@Corresponding author E-mail: dubinina.t.vid@gmail.com

*Synthetic approach to a new substituted tetrathieno[2,3-*b*]porphyrazine, its planar and sandwich-type complexes was developed. Aggregation phenomena and spectral properties of the target compounds were investigated by UV-Vis spectroscopy and AFM. Electrochemical behaviour of the Zn complex was studied in a wide range of potentials (-2.0÷2.0 V). The NLO properties of Zn complex was studied by the z-scan approach.*

Keywords: Porphyrazines, nonlinear optical properties, electrochemistry, sandwich-type complexes, UV-Vis spectroscopy.

Introduction

Tetrathieno[2,3-*b*]porphyrazines are the less studied analogues of phthalocyanines.^[1] The presence of a sulphur-containing heterocyclic moiety in the macrocycle improves photoconductivity^[2] and nonlinear optical (NLO) properties.^[3] Therefore such compounds are of importance for a range of functional applications including photovoltaic cells,^[2b] photodynamic therapy (PDT),^[4] and optical data storage devices.^[5] Previously reported unsubstituted tetrathieno[2,3-*b*]porphyrazines exhibit low solubility in organic solvents, and the synthetic strategy is inefficient (yield ≤ 16%).^[6] Synthesis of alkoxy-substituted porphyrazines is also of low yield (15-20 %) and includes a complicated synthesis of initial dinitrile.^[2a] The present paper focuses on the synthesis of highly-soluble substituted tetrathieno[2,3-*b*]porphyrazines and investigation of spectral and electrochemical properties.

Experimental

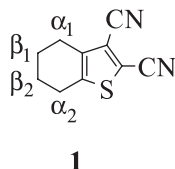
Column chromatography was carried out on neutral MN-Aluminiumoxid. Preparative TLC was performed using Merck Aluminium Oxide F₂₅₄ neutral flexible plates. The electrolyte [Bu₄N]⁺[BF₄]⁻ (Sigma-Aldrich) was recrystallized twice from ethyl acetate/hexane (9:1, V/V) and dried under vacuum at 70 °C. *o*-Dichlorobenzene (DCB, 99%, Sigma-Aldrich, HPLC-grade) for voltammetric and spectroelectrochemical studies was used as received. All other reagents and solvents were obtained or distilled according to standard procedures. The salts Mg(OAc)₂·4H₂O; Zn(OAc)₂·4H₂O; Lu(OAc)₃·4H₂O was dried immediately before use in a vacuum desiccator for 4 h at 90 °C. All reactions were TLC and UV/Vis controlled until complete disappearance of the starting reagents if not additionally specified.

Electronic absorption (UV-Vis) spectra were recorded on a ThermoSpectronic Helios- α spectrophotometer using quartz cells (0.5×1cm). MALDI-TOF mass spectra were taken on a VISION-2000 mass spectrometer with 2-[(2E)-3-(4-*tert*-butylphenyl)-2-methylprop-2-enylidene]-malonitrile (DCTB) as the matrix. High resolution MALDI mass spectra were registered on a Bruker ULTRAFLEX II TOF/TOF instrument with DCTB as the matrix. ¹H and ¹³C NMR spectra were recorded on a Bruker "Avance 400" spectrometer (400.13 and 100.61 MHz respectively) at 20°C (if not additionally specified). Chemical shifts are given in ppm relative to SiMe₄.

Electrochemical measurements were carried out using IPC-Pro (Econix, Moscow, Russia) and EmStat (Palm Instrument BV, Utrecht, the Netherlands) potentiostats. Cyclic voltammetry (CVA) and square-wave voltammetry (SWVA) were performed in a conventional three electrode cell using Pt-disk (2.0 mm in diameter) working and Pt-foil counter electrodes. A calomel reference electrode (SCE, 3M NaCl) was connected to the solution through a salt-bridge and a Luggin capillary, whose tip was placed close to the working electrode. The junction potentials were corrected by ferrocenium⁺/ferrocene (Fc⁺/Fc) couple each time after a series of measurements ($E_{1/2}(\text{Fc}^+/\text{Fc}) = 0.592 \text{ V}$). Freshly distilled dichloromethane (purium, Reachim Russia) and *o*-dichlorobenzene (DCB, 99% Sigma-Aldrich, HPLC-grade) freshly passed through an Al₂O₃ layer were used as solvents, and 0.15 M solution of Bu₄NBF₄ (Sigma-Aldrich, dried under vacuum at +80°C) in *o*-dichlorobenzene containing (2÷10)·10⁻⁴ M of sample was bubbled with argon for 20 min before measurements. Blank voltammograms were recorded in the same background solution.

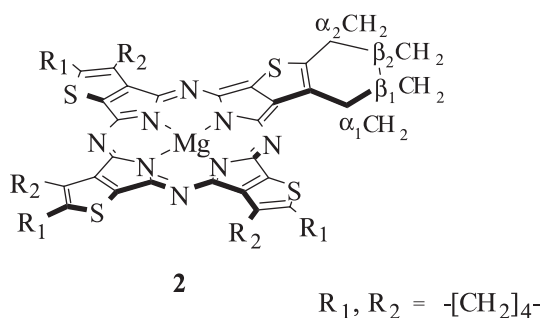
AFM studies were carried out by means of a Solver-P47H (NT-MDT) microscope. Tapping mode and a high accuracy composite silicon/polysilicon HA_NC probe for non-contact AFM were applied to obtain images. Menzel-Gläser cover slips (18×18 mm) were employed as the substrate. The rounding-off radius of the probe was less than 10 nm.

2-Iodo-4,5,6,7-tetrahydrobenzo[*b*]thiophene-3-carbonitrile was synthesized according to the published procedures.^[6,7]

4,5,6,7-Tetrahydrobenzo[*b*]thiophene-2,3-dicarbonitrile (**1**).

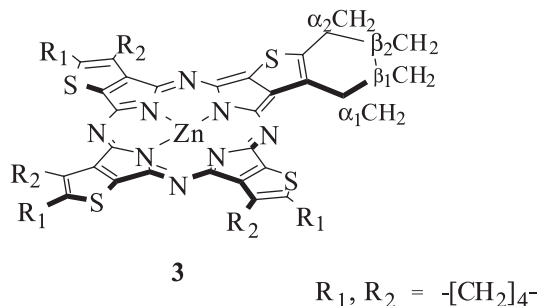
A mixture of 2-iodo-4,5,6,7-tetrahydrobenzo[*b*]thiophene-3-carbonitrile (2.400 g, 8.3 mmol) and CuCN (1.850 g, 0.020 mol) were refluxed in DMF (40 ml) for 10 h (TLC-control: Al₂O₃, C₆H₆: *n*-hexane (1:1 V/V)). The reaction mixture was cooled to room temperature and water was added. The product was collected by extraction with dichloromethane. The organic layer was dried with CaCl₂. The solvent was evaporated and the resulting solid was purified twice by column chromatography (Al₂O₃, CHCl₃). This yielded **1** as a pale yellow solid (1.020 g, 64%). mp 82.6°C (lit.^[6] 82–83°C), $R_f=0.4$ (Al₂O₃, C₆H₆: *n*-hexane (1:1 V/V)), ¹H NMR (400 MHz, CDCl₃) δ_H ppm: 1.85–1.93 (m, 4H, $\beta_{1,2}$ -CH₂), 2.73 (t, $J=5.7$ Hz, 2H, α_1 -CH₂), 2.81 (t, $J=5.7$ Hz, 2H, α_2 -CH₂). ¹³C NMR (100 MHz, CDCl₃) δ_C ppm: 21.38, 22.39 ($\beta_{1,2}$ -CH₂), 24.36, 25.22 ($\alpha_{1,2}$ -CH₂), 111.60 and 111.93 (CN), 113.70 (C2), 119.47 (C3), 138.39 (C4), 145.71 (C5).

2,3,8,9,14,15,20,21-Octakis[4',5',6',7'-tetrahydrobenzo]-tetra-2,3-thiophenophorphyrazine magnesium (**2**).



A mixture of **1** (0.200 g, 1.064 mmol), Mg(OAc)₂·4H₂O (0.143 g, 0.668 mmol) and lithium methoxide (0.019 g, 0.500 mmol) were refluxed in *n*-octanol (3.5 ml) for 8 h (TLC-control: Al₂O₃, C₆H₆). The reaction mixture was cooled to room temperature and a mixture MeOH:H₂O (10:1 V/V) was added. A dark green precipitate was filtered and washed with water and MeOH. This yielded **2** (0.093 g, 45%). UV-Vis (THF) λ_{max} nm (lg ϵ): 663 (4.49), 639 (3.98), 603 (3.77), 369 (4.35). ¹H NMR (400 MHz, CDCl₃:MeOH 100:1 V/V) δ_H ppm: 1.77 (m, 16H, $\beta_{1,2}$ -CH₂), 2.65–2.70 (m, 16H, $\alpha_{1,2}$ -CH₂). MS-MALDI-TOF m/z : 776 ([M]⁺, 100%).

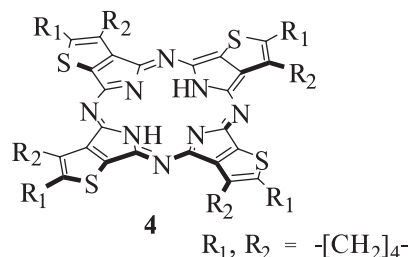
2,3,8,9,14,15,20,21-Octakis[4',5',6',7'-tetrahydrobenzo]-tetra-2,3-thiophenophorphyrazine zinc (**3**).



A mixture of **1** (0.070 g, 0.370 mmol), Zn(OAc)₂·4H₂O (0.047 g, 0.185 mmol) and lithium methoxide (0.007 g, 0.185 mmol) were refluxed in *n*-octanol (1.5 ml) for 5 h (TLC-control:

Al₂O₃, C₆H₆). The reaction mixture was cooled to room temperature and a mixture MeOH:H₂O (10:1 V/V) was added. A dark green precipitate was filtered and washed with water and MeOH. This yielded **3** (0.061 g, 80%). UV-Vis (THF) λ_{max} nm (lg ϵ): 665 (4.6), 603 (3.9), 367 (4.4). ¹H NMR (400 MHz, Py-d₅) δ_H ppm: 2.02 (m, 8H, β_2 -CH₂), 2.08 (m, 8H, β_1 -CH₂), 3.11–3.16 (m, 8H, α_2 -CH₂), 3.84–3.98 (m, 8H, α_1 -CH₂). HRMS-MALDI-TOF/TOF m/z : [M]⁺ calculated for C₄₀H₃₄N₈S₄Zn: 818.4057; found: 818.4082.

2,3,8,9,14,15,20,21-Octakis[4',5',6',7'-tetrahydrobenzo]-25*H*,27*H*-tetra-2,3-thiophenophorphyrazine (**4**).

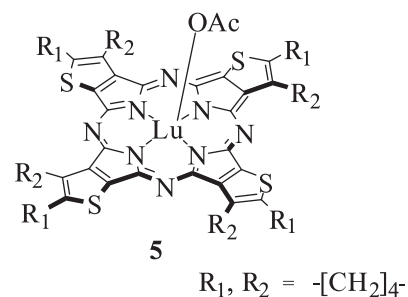


a) Approach with concentrated sulfuric acid. The magnesium complex **2** (0.011 g, 0.014 mmol) was dissolved in concentrated sulfuric acid (3 ml). This solution was poured into the ice. At the same time the green precipitate was formed. This precipitate was filtered and washed with water and MeOH to give **4** (0.004 g, 38%). UV-Vis (THF) λ_{max} nm (lg ϵ): 699 (4.60), 655 (4.54), 352 (4.55). HRMS-MALDI-TOF/TOF: m/z [M]⁺ calculated for C₄₀H₃₄N₈S₄: 754.2912 [M]⁺; found: 754.3190.

b) Approach with concentrated trifluoroacetic acid. The magnesium complex **2** (0.011 g, 0.014 mmol) was dissolved in concentrated trifluoroacetic acid (3 ml). This solution was poured into the ice. At the same time the green precipitate was formed. This precipitate was filtered and washed with water and MeOH to give **4** (0.005 g, 48%). The characteristics were identical with those obtained by method (a).

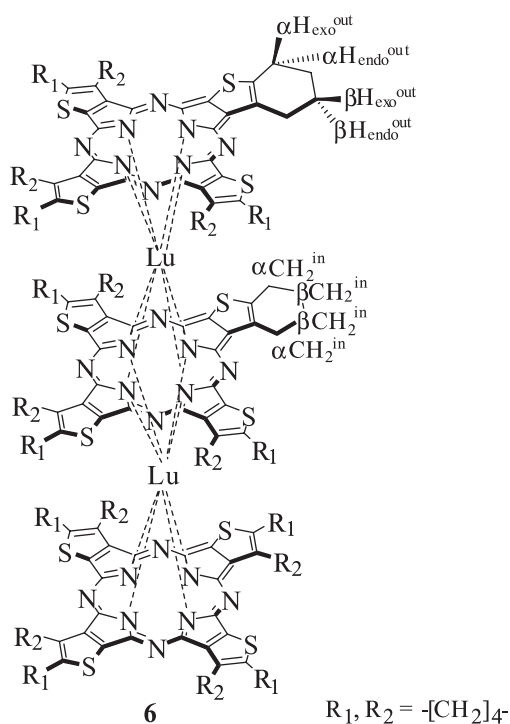
c) Approach with pyridine hydrochloride. A mixture of **3** (0.030 g, 0.0370 mmol) and pyridine hydrochloride (0.012 g, 0.10 mmol) were refluxed in pyridine (600 μ l) for 3 h. The reaction mixture was cooled to room temperature and a mixture MeOH:H₂O (10:1 V/V) was added. A dark green precipitate was filtered and washed with water and MeOH. This yielded **4** (0.026 g, 93%). The characteristics were identical with those obtained by method (a).

2,3,8,9,14,15,20,21-Octakis[4',5',6',7'-tetrahydrobenzo]-tetra-2,3-thiophenophorphyrazinatoluthetium acetate (**5**).



A mixture of **4** (12 mg, 0.016 mmol), Lu(OAc)₃·4H₂O (3 mg, 0.007 mmol) and lithium methoxide (0.004 g, 0.105 mmol) were heated in the mixture TCB:C₁₆H₃₃OH (1:1 V/V; V_{total} = 300 μ l) at the temperature range: 190–230°C for 2.5 h (TLC-control: Al₂O₃, C₆H₆). The reaction mixture was cooled to room temperature and a mixture MeOH:H₂O (5:1 V/V) was added. A dark green precipitate was filtered and washed with water and MeOH. The compound **5** was separated using preparative TLC (Al₂O₃, C₆H₆). This yielded **5** (0.010 g, 63%). $R_f=0.3$ (Al₂O₃, C₆H₆). UV-Vis (THF) λ_{max} nm (lg ϵ):

664 (4.53), 604 (3.98), 362 (4.43). HRMS-MALDI-TOF/TOF: m/z [M-OAc-H]⁺ calculated for C₄₀H₃₁LuN₈S₄: 926.0962; found: 926.0688.



Tris[2,3,8,9,14,15,20,21-octakis[4',5',6',7'-tetrahydrobenzo]tetra-2,3-thiophenophorphyrazine] dilutetium (**6**) was separated using preparative TLC (Al₂O₃, C₆H₆). This yielded **6** (0.005 g, 36%). R_f=0.8 (Al₂O₃, C₆H₆). UV-Vis (THF) λ_{max} nm (lgε): 698 (3.85), 656 (4.59), 551 (3.67), 371 (4.45), 310 (4.37). ¹H NMR (400 MHz, CDCl₃) δ_H ppm: 1.96 (m, 16H, β-H_{exo}^{out}), 2.09 (m, 16H, β-H_{endo}^{out}), 2.32 (m, 16H, β-Hⁱⁿ), 2.60 (m, 16H, α-H_{exo}^{out}), 2.84 (m, 16H, α-H_{endo}^{out}), 3.55 (m, 16H, α-Hⁱⁿ). HRMS (MALDI-TOF/TOF) m/z : [M]⁺ calculated for C₁₂₀H₉₆Lu₂N₂₄S₁₂: 2608.9210; found: 2608.8909.

Results and Discussion

4,5,6,7-Tetrahydrobenzo[*b*]thiophene-2,3-dicarbonitrile was chosen as the starting compound. This dinitrile was obtained by a standard synthetic route.^[6,7] Replacement of 1,1,3,3-tetramethylurea^[6] by DMF at the stage of cyanation allowed for an increase in yield from 47 to 64%. According to the literature data,^[6] tetrathieno[2,3-*b*]porphyrazines can exist as a mixture of four possible isomers (excluding the isomers of cyclohexene moieties), C_{4h}, C_s, D_{2h} and C_{2v}, which cannot be separated. Four similar randomers also occur for 1,2-naphthalocyanines.^[8,9]

The porphyrazine complexes were synthesised from the dinitrile **1** and acetates of corresponding metals in boiling *n*-octanol upon addition of lithium methoxide base (Scheme 1). Magnesium and zinc ions were chosen for the subsequent formation of ligands.^[10] Formation of porphyrazines was not observed under mild conditions in a boiling isoamyl alcohol. Metal-free porphyrazine was obtained by the method described for phthalocyanine ligands,^[10c,11] which involved treatment of magnesium complex **2** with strong concentrated acids (Scheme 1). However, partial destruction of thiophene moieties under polymerisation in concentrated acid led to a low yield of target compound.

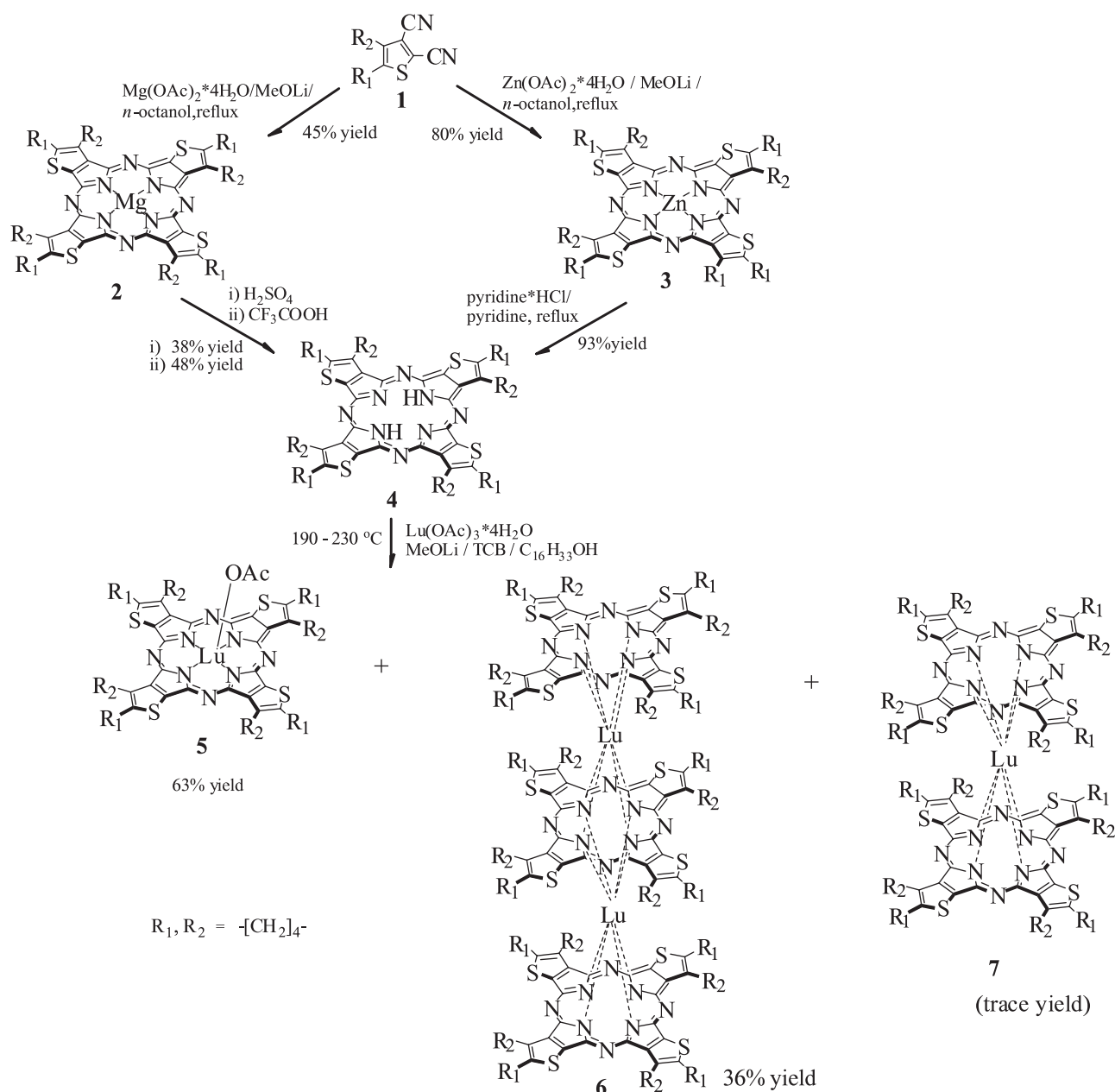
Treatment of magnesium complex **2** with a weaker acetic acid did not yield **4**. Demetallation was done under mild conditions, as recently reported for zinc phthalocyanines. This approach includes a reaction between zinc complex and pyridine hydrochloride in boiling pyridine and is based on formation of a ternary pyridine–Zn–Pc complex with square pyramidal zinc coordination.^[10a] Present work is the first successful example of the synthesis of porphyrazine compounds by such route.

Phthalocyanine and porphyrazine complexes of rare earth elements (REE) find a large range of applications in optics and electronics.^[12] In light of that, we have chosen to synthesize a lutetium complex of **4** as our first example. Tetrathieno[2,3-*b*]porphyrazine lutetium **5** was obtained by a reaction of ligand **4**, lutetium acetate and lithium methoxide in the mixture of cetyl alcohol and TCB (1:1 volume ratio) (Scheme 1).

Substituted triple-decker lutetium porphyrazine **6** was separated as a by-product in the synthesis of **5**. Noteworthy, this is the first example of sandwich-type porphyrazine with annelated heterocyclic ring. Formation of the double-decker complex **7** was confirmed by MALDI TOF mass spectrometry, but all attempts to isolate the product were unsuccessful. Perhaps, this is due to the low stability of π-radical thienoporphyrazine structures. Even the standard synthetic route (Lu acetylacetonate; lithium methoxide; 190°C; *n*-octanol)^[13] did not yield double-decker complex. Novel porphyrazines **2–6** were characterized by high resolution MALDI-TOF mass spectrometry, UV-Vis and ¹H NMR spectroscopy.

UV-Vis spectra of the obtained porphyrazines are very instructive. Metal-free **4** exhibits *Q*-band splitting (Figure 1a), that can be attributed to the non-degenerated LUMO orbital.^[14] In contrast, *Q*-bands in complexes **2, 3, 5** were not split (Figure 1 and Table 1). This result is in accord with the literature data^[15] and DFT calculations^[14] for porphyrazines. The absence of *Q*-band splitting and the values of full width at half maximum (FWHM) for porphyrazine complexes in THF (Table 1.) allow to conclude that C_{4h} and C_{2v} randomers^[9] predominate in the mixture. A weak intensity broad band, which is characteristic for phthalocyanines and porphyrazines that containing chalcogenide atoms, was observed in the range of 400–450 nm. This band refers to the charge transfer from thiophene cycles to porphyrazine core.^[3a] Compared to unsubstituted thieno[2,3-*b*]porphyrazine,^[6] *Q*-bands for tetrahydrobenzo substituted complexes are bathochromically shifted. This phenomenon can be explained by the donor effect of substituents. Nature of the central metal in porphyrazine complexes did not influence the *Q*-band position (Figure 1), as was also the case for monophthalocyanines and naphthalocyanines.^[11] *Q*-band of the metal-free compound **4** had a bathochromic shift with respect to *Q*-bands of complexes **2, 3** and **5**. The triple-decker complex **6** exhibits *Q*-band splitting and a hypsochromic shift of the main absorption maximum as compared to those of monoporphyrazines. Similar features have been previously reported for triple-decker phthalocyanine complexes^[16,17] and are due to the interaction of the inner and external deck.^[13]

The spectra of porphyrazines **2–5** in a non-coordinating solvent (C₆H₆) exhibit aggregation behaviour that is



Scheme 1. Synthesis of thienoporphyrazine complexes **2-7** (the structures of complexes are shown for one isomer).

manifested in broadening of Q -bands and decreasing of the Q -band: B -band intensity ratio I/I_{\max} (Table 1). Due to the steric effect of external decks the aggregation was minimal in the case of the triple-decker compound **6**.

The aggregation effect was stronger in solid films of **6**. Films possessed an “island-type”, large-grain structure (Figure 2). Grain size depended on the coordination effect of the solvent. In the case of C_6H_6 the grain size was 45 nm in height and 200 nm in width. For highly-coordinating THF, grain size was 7 nm in height and from 60 to 80 nm in width.

Electrochemical behaviour of complex **3** in *o*-DCB was investigated (Figure 3). The square-wave voltammogram (SWVA) exhibited three reduction potentials at -0.915, -1.295 and -1.735 V and two oxidation potentials at +0.835 and +1.520 V. In cyclic voltammogram (CVA), only highly-reversible redox processes Red_1 , Red_2 and Ox_1 were

observed, which is likely due to the lower sensitivity of the method. Under the potential scanning until 1.6 V and higher, poor reversibility of the Ox_2 process resulted in a decrease of intensity and a shift of the reverse peak of Ox_1 .

Investigation of nonlinear optical properties was carried out using a well known Z-scan technique.^[18] The scheme of the experiment is presented in Figure 4.

In our study we used a Nd:YAG laser operated at the TEM₀₀ mode with the pulse duration of $\tau_p = 350$ ps (halfwidth at e^{-1} intensity) at the repetition rate of 5 Hz. To obtain the second harmonic at 532 nm we used an ADP-crystal. The beam was tightly focused and the beam radius (halfwidth at e^{-2} intensity) was $\omega_0 = 30 \mu m$ at the focus. The energy of the pulse was $E_0 = 38 \mu J$. Measurements with closed aperture help to reveal the characteristics of the nonlinear refraction. The measurements with open aperture reveal the characteristics of the non-linear absorption.

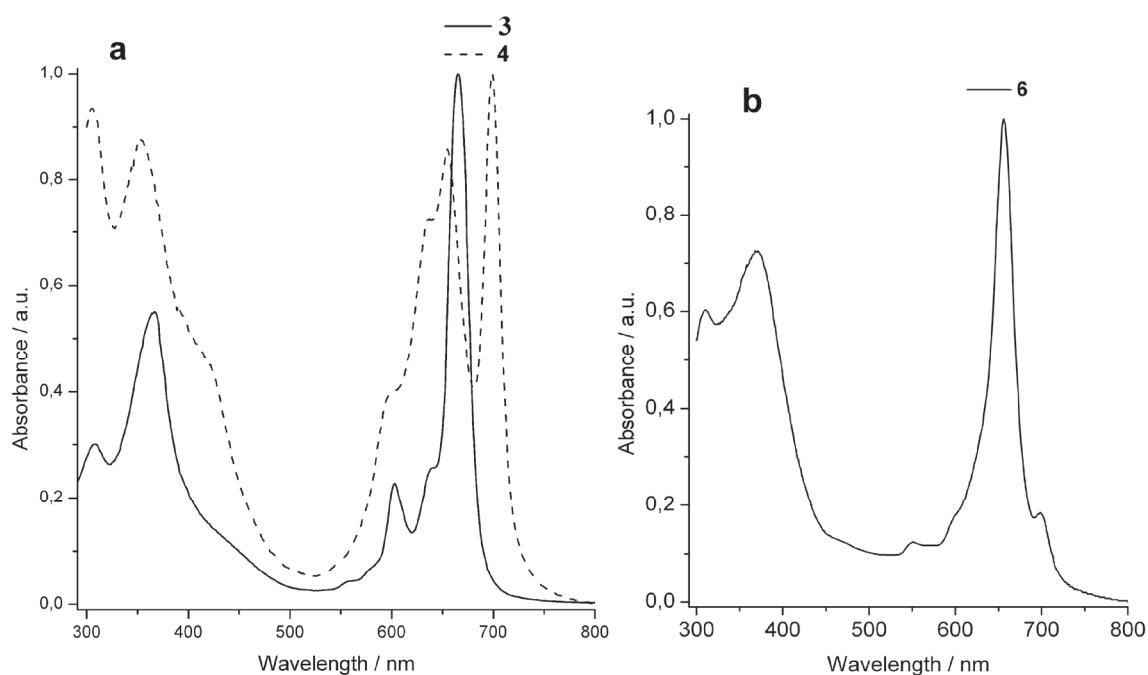


Figure 1. UV-Vis spectra of thienoporphyrazines **3**, **4** and **6** in THF.

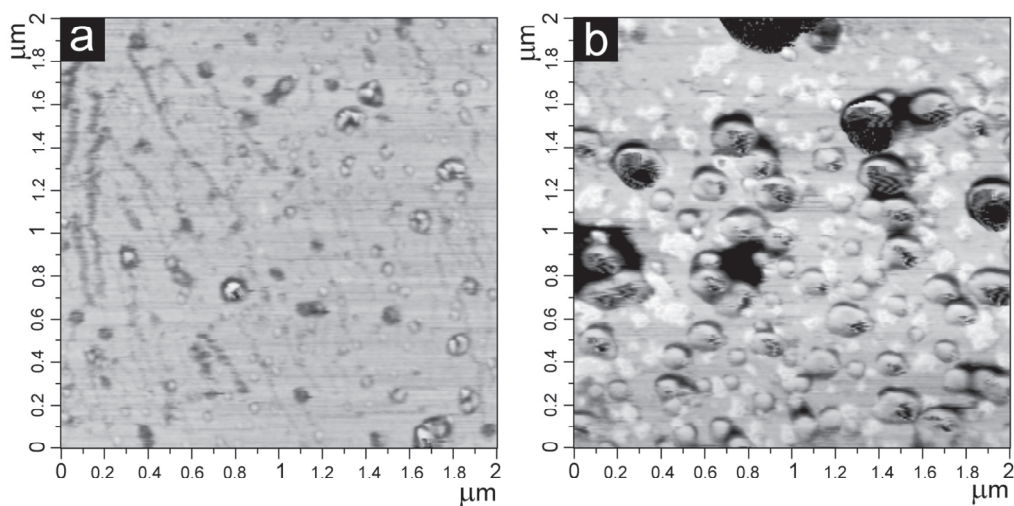


Figure 2. AFM phase contrast images of thin films of compound **6** deposited from a THF solution (a) and from a C_6H_6 solution (b) ($C = 10^{-6}$ M).

Table 1. UV-Vis spectral data for compounds **2-6**.

Compound	λ (I/I_{max}), nm in THF	λ (I/I_{max}), nm in C_6H_6	Full Width at Half Maximum (FWHM) for Q -band (nm) in THF	Full Width at Half Maximum (FWHM) for Q -band (nm) in C_6H_6
2	663 (1.00); 639 (0.31); 603 (0.19); 369 (0.77)	668 (0.83); 611 (0.24); 373 (1.00); 306 (0.59)	20 (663)	27 (668)
3	665 (1.00); 603 (0.23); 367 (0.55)	672 (1.00); 641 (0.42); 619 (0.41); 363(0.94); 310 (0.57)	21 (665)	26 (672)
4	699 (1.00); 655 (0.86); 352 (0.88)	700 (0.92); 656 (0.87); 638 (0.80); 358 (1.00); 312 (0.78)	15 (699)	16 (700)
5	664 (1.00); 604 (0.28); 362 (0.79)	667 (0.97); 605 (0.34); 363 (1.00); 305 (0.88)	20 (664)	26 (667)
6	698 (0.18); 656 (1.00); 551 (0.12); 371 (0.72); 310 (0.60)	697 (0.19); 655 (1.00); 550 (0.15); 371 (0.81); 314 (0.60)	19 (698)	20 (655)

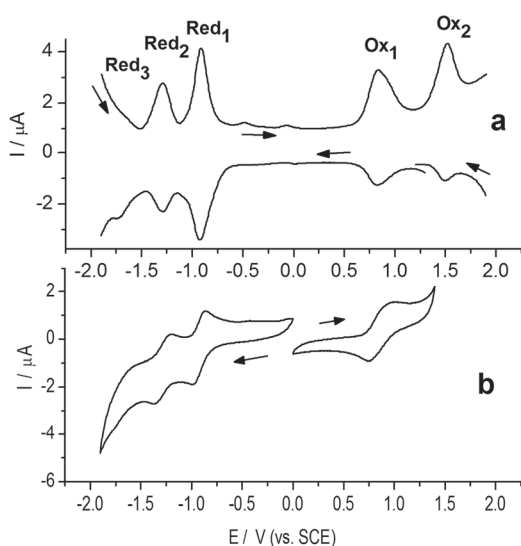


Figure 3. Square wave (a) and cyclic (b) voltammograms of **3** in *o*-DCB.

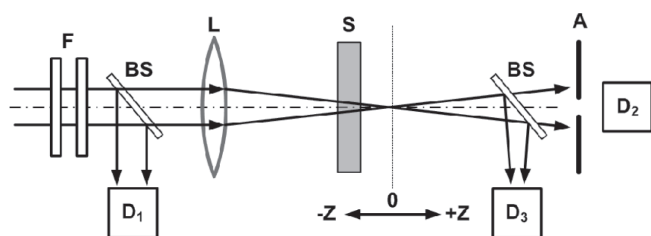


Figure 4. The Z-scan setup. F- filters, BS - beam splitter, D_1 , D_2 and D_3 are photodetectors, A - aperture, S - sample.

Table 2. NLO measurements data for compound **3**.

Compound	$Re\chi^{(3)}$ (esu)	$Im\chi^{(3)}$ (esu)	λ (nm)	I (GW/cm ²)
26	$3.45 \cdot 10^{-14}$	$11.5 \cdot 10^{-14}$	532	2.5

Here we present the best result, which was reached for Zn complex. In Table 2 there are the real part of nonlinear

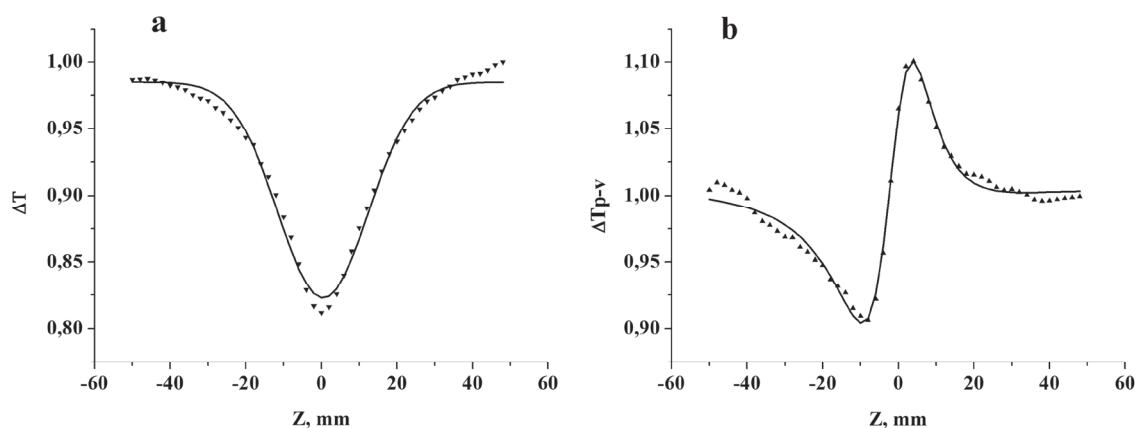


Figure 5. An open (a) and closed (b) aperture Z-scans measured for Zn complex in C_6H_6 ($C = 6 \cdot 10^{-5}$ M).

optical susceptibility, corresponded to nonlinear refraction, and the imaginary part of nonlinear optical susceptibility, corresponded to nonlinear absorption. This compound possesses the negative nonlinearity (Figure 5), which increases under the increase in the concentration of target compound in solution. Noteworthy, that metal-free and triple-decker compounds did not show remarkable nonlinearity for the similar concentrations.

As one can see from the open-aperture z-scan (Figure 5a) the sample shows reverse saturable absorption. To interpret the experimental data it is convenient to use the five-level model. The five-level model is represented with the Jablonski diagram which describes processes of excitation and relaxation in the molecule. In this model commonly only one-photon processes are considered. The scheme of the model is presented in Figure 6. The ground state is signed as S_0 .

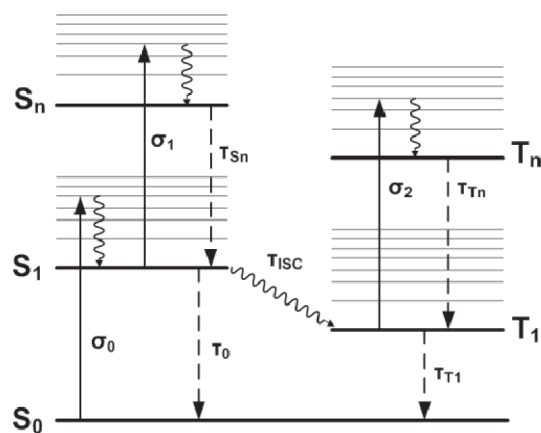


Figure 6. Jablonski diagram of excitation and relaxation processes in a molecule.^[19]

Absorption of the photon at 532 nm leads to the transition of the electron to the vibronic sublevel of the first excited singlet state S_1 . The lifetime of the vibronic sublevel is of subpicosecond range, so only the direct transition $S_0 \rightarrow S_1$ can be considered. The electrons from S_1 can relax either to the ground state, with the lifetime τ_0 , or to the triplet state T_1 via intersystem crossing, with the

lifetime τ_{ISC} . Under the influence of the incident radiation excited electrons at states S_1 and T_1 will transit to upper excited states S_n and T_n , respectively. The population dynamics of all mentioned states is described by system of rate equations:

$$\frac{dN_0}{dt} = -\sigma_0 N_G \frac{I}{\hbar\omega} + \frac{N_{S1}}{\tau_0} + \frac{N_{T1}}{\tau_{T1}}$$

$$\frac{dN_{S1}}{dt} = \sigma_0 N_G \frac{I}{\hbar\omega} - \sigma_1 N_{S1} \frac{I}{\hbar\omega} - \frac{N_{S1}}{\tau_0} - \frac{N_{S1}}{\tau_{ISC}} + \frac{N_{S2}}{\tau_{S2}}$$

$$\frac{dN_{S2}}{dt} = \sigma_1 N_{S1} \frac{I}{\hbar\omega} - \frac{N_{S2}}{\tau_{S2}}$$

$$\frac{dN_{T1}}{dt} = -\sigma_2 N_{T1} \frac{I}{\hbar\omega} + \frac{N_{S1}}{\tau_{ISC}} + \frac{N_{T2}}{\tau_{T2}} - \frac{N_{T1}}{\tau_{T1}}$$

$$\frac{dN_{T2}}{dt} = \sigma_2 N_{T1} \frac{I}{\hbar\omega} - \frac{N_{T2}}{\tau_{T2}}$$

where N_i is the population of the i -th state, σ_0 is the ground state absorption cross-section, σ_1 is the first excited singlet state absorption cross-section, σ_2 is the first excited triplet state absorption cross-section, τ_i is the lifetime of the i -th state and τ_{ISC} is the intersystem crossing lifetime. The absorption in the sample is governed by the Beer's law:

$$\frac{dI}{dz'} = -\sigma_0 I N_G - \sigma_1 I N_{S1} - \sigma_2 I N_{T1}$$

where z' is the coordinate inside the sample. Where the first term describes the absorption of the ground state and the other two describe the absorption of excited singlet and triplet state, respectively. The transmittance of the pulse is determined by the formula

$$T(z) = \frac{\int_{-\infty}^{\infty} dt \int_0^{\infty} I_{out}(r, z, t) r dr}{\int_{-\infty}^{\infty} dt \int_0^{\infty} I_{in}(r, z, t) r dr}$$

where I_{in} and I_{out} are the intensities of incident and transmitted pulses, respectively. Calculating transmittance for each z -position yields the z -scan curve.

The results we present in the Table 2 are calculated with the $\chi^{(3)}$ - formalism which doesn't describe full nature of the processes which take place during the illumination with intense laser pulse. It is necessary to use the five-level model. However, using of the model implies that lifetimes of the excited states are known. To calculate the values of σ_1 and σ_2 time-resolved measurements are needed. These measurements are very important to characterize

the nonlinear optical properties and they are the subject of further investigation.

Conclusions

In conclusion, novel highly-soluble substituted porphyrazines were synthesised in high yields (45-80%). The synthetic route to the thieno[2,3-*b*]porphyrazine complexes as a perspective building-blocks for sandwich-type porphyrazines was developed. Heterocyclic ring annelated sandwich-type porphyrazine complex was synthesised for the first time. Spectral properties and aggregation phenomena of target compounds were investigated by UV-Vis and AFM techniques. Electrochemical behaviour of the Zn complex was studied by CVA and SWWA and the presence of reversible redox processes was shown. The presence of induced absorption shows, that Zn complex can be used as an optical limiter.

Acknowledgements. The research was supported by the Russian Foundation for Basic Research (Grant No. 08-03-00753), and the programme of the Presidium of the Russian Academy of Science "Development of a strategy of organic synthesis and creation of compounds with valuable and applied proprieties".

References

1. Linstead R.P., Noble E.G., Wright J.M. *J. Chem. Soc.* **1937**, 911-921.
2. (a) Klawby D.M., Swager T.M. *Chem. Mater.* **1997**, *9*, 535-538. (b) Miyoshi Y., Fujimoto T., Yoshikawa H., Matsushita M.M., Awaga K., Yamada T., Ito H. *Org. Electron.* **2011**, *12*, 239-243. (c) Du C., Guo Y., Liu Y., Qiu W., Zhang H., Gao X., Liu Y., Qi T., Lu K., Yu G. *Chem. Mater.* **2008**, *20*, 4188-4190.
3. (a) Taraymovich E.S., Korzhenevskii A.B., Mitasova Y.V., Kumeev R.S., Koifman O.I., Stuzhin P.A. *J. Porphyrins Phthalocyanines* **2011**, *15*, 54-65. (b) Cook M.J., Jafari-Fini A. *Tetrahedron* **2000**, *56*, 4085-4094.
4. Brown S.B., Brown E.A., Walker I. *Lancet Oncol.* **2004**, *5*, 497-508.
5. (a) Luo Q., Liu Y., Tian H., Photochromic Dithienylethene-Phthalocyanines and Their Analogs. In: *Functional Phthalocyanine Molecular Materials* (Jiang, J., Ed). Berlin Heidelberg: Springer-Verlag: Berlin, **2010**; Vol. 135, 89-103; (b) de la Torre G., Claessens C. G., Torres T. *Chem. Commun. (Cambridge, U. K.)* **2007**, 2000-2015.
6. Christie R.M., Freer B.G. *Dyes Pigm.* **1997**, *33*, 107-118.
7. Gewald K., Schinke E., Bottcher H. *Chem. Ber.* **1966**, *99*, 94-100.
8. Hanack M., Renz G., Strähle J., Schmid S. *Chem. Ber.* **1988**, *121*, 1479-1486.
9. Negrimovskii V.M., Bouvet M., Luk'yanets E.A., Simon J. *J. Porphyrins Phthalocyanines* **2000**, *4*, 248-255.
10. (a) Alzeer J., Roth P.J.C., Luedtke N.W. *Chem. Commun. (Cambridge, U. K.)* **2009**, 1970-1971. (b) Dubinina T.V., Trashin S.A., Borisova N.E., Boginskaya I.A., Tomilova L.G., Zefirov N.S. *Dyes Pigm.* **2012**, *93*, 1471-1480. (c) Dubinina T.V., Ivanov A.V., Borisova N.E., Trashin S.A., Gurskiy S.I., Tomilova L.G., Zefirov N.S. *Inorg. Chim. Acta* **2010**, *363*, 1869-1878.
11. Dubinina T.V., Piskovoi R.A., Tolbin A.Y., Pushkarev V.E., Vagin M.Y., Tomilova L.G., Zefirov N.S. *Russ. Chem. Bull.* **2008**, *57*, 1912-1919.

New Substituted Tetrathieno[2,3-b]porphyrazines

12. Abdurrahmanoglu S., Altindal A., Riza Ozkaya A., Bulut M., Bekaroglu O. *Chem. Commun. (Cambridge, U. K.)* **2004**, 2096-2097.
13. Pushkarev V.E., Breusova M.O., Shulishov E.V., Tomilov Y.V. *Russ. Chem. Bull.* **2005**, 54, 2087-2093.
14. Kobayashi N., Nakajima S.-I., Ogata H., Fukuda T. *Chem.--Eur. J.* **2004**, 10, 6294-6312.
15. Linstead R.P., Whalley M. *J. Chem. Soc.* **1952**, 4839-4846.
16. Martynov A.G., Zubareva O.V., Gorbunova Y.G., Sakharov S.G., Nefedov S.E., Dolgushin F.M., Tsivadze A.Y. *Eur. J. Inorg. Chem.* **2007**, 2007, 4800-4807.
17. Zhu P., Pan N., Li R., Dou J., Zhang Y., Cheng D.Y.Y., Wang D., Ng D.K.P., Jiang J. *Chem.--Eur. J.* **2005**, 11, 1425-1432.
18. Sheik-Bahae M., Said A.A., Wei T.-H., Hagan D. J., Van Stryland E.W. *IEEE J. Quantum Electron.* **1990**, 26, 760-769.
19. Li C., Zhang L., Yang M., Wang H., Wang Y. *Physical Review A* **1994**, 49, 1149-1157.

Received 08.06.2012

Accepted 18.06.2012